The use of RGB Imaging and FTIR Sensors for Mineral mapping in the Reiche Zeche underground test mine, Freiberg

Desta, Feven; Buxton, Mike

Publication date
2017

Document Version
Final published version

Published in
2017 REAL TIME MINING - Conference on Innovation on Raw Material, Amsterdam, The Netherlands

Citation (APA)
Desta, F., & Buxton, M. (2017). The use of RGB Imaging and FTIR Sensors for Mineral mapping in the Reiche Zeche underground test mine, Freiberg. In J. Benndorf , M. Buxton, D. Hößelbarth, & T. van Gerwe (Eds.), *2017 REAL TIME MINING - Conference on Innovation on Raw Material, Amsterdam, The Netherlands : Amsterdam, The Netherlands , 10th & 11th October 2017* (pp. 103-127)

The use of RGB Imaging and FTIR Sensors for Mineral mapping in the Reiche Zeche underground test mine, Freiberg

Feven S. Desta, Mike W.N. Buxton

Resource Engineering, Delft University of technology, Stevinweg 1, 2628 CN Delft, The Netherlands

ABSTRACT

The application of sensor technologies for raw material characterization is rapidly growing, and innovative advancement of the technologies is observed. Sensors are being used as laboratory and in-situ techniques for characterization and definition of raw material properties. However, application of sensor technologies for underground mining resource extraction is very limited and highly dependent on the geological and operational environment. In this study the potential of RGB imaging and FTIR spectroscopy for the characterization of polymetallic sulphide minerals in a test case of Freiberg mine was investigated. A defined imaging procedure was used to acquire RGB images. The images were georeferenced, mosaicked and a mineral map was produced using a supervised image classification technique. Five mineral types have been identified and the overall classification accuracy shows the potential of the technique for the delineation of sulphide ores in an underground mine. FTIR data in combination with chemometric techniques were evaluated for discrimination of the test case materials. Experimental design was implemented in order to identify optimal pre-processing strategies. Using the processed data, PLS-DA classification models were developed to assess the capability of the model to discriminate the three material types. The acquired calibration and prediction statistics show the approach is efficient and provides acceptable classification success. In addition, important variables (wavelength location) responsible for the discrimination of the three materials type were identified.

1 Introduction

The future challenges in mining can be attributed to depletion of known shallow mineral reserves, and limited exploration of deep (>400m depth) resources. Future mining is moving to extraction of valuable materials under geologically more complex conditions. Geologically complex conditions are exemplified by deeper mines, a low continuity in grade, presence of toxic elements and high irregularity in the geometry of the ore boundaries. Mining in complex conditions requires novel technique and a real-time framework for advanced data acquisition and resource model updating

[1]. Advanced data acquisition to provide relevant data for real-time online process control and optimization in mining application can be achieved using sensor technologies.

The applicability of sensor technologies for insitu material characterization is very limited. The limited use of sensors for insitu material characterization is attributed to various factors. For example, additional work is needed to show the added value of the use of sensors in the mining industry; the design of some of the technologies are only intended for laboratory applications, sensor choice is very specific to material/ deposit type and dependent on the sensor type, the initial investment to purchase (and setup) the instrument might be higher than the benefit to be realized.

In spite of the limited use of sensors in the mining industry; studies [2] [3] [4] indicate that, the use of sensor technologies in the mining industry will result in improved efficiency; increase productivity and safety, reduce operational cost and environmental impact.

Sensor technologies provide data on different aspects of material properties. Fundamental understanding of material characteristics is crucial in selecting the appropriate sensor solutions for material discrimination. Material property is a broad term which addresses different properties of a certain material; these properties include physical, chemical, optical, mechanical and atomic properties. Sensor technologies can be applied throughout the mining value chain; it can be applied during extraction at the mining face, during material handling and processing. This study presents the results of RGB Imaging and FTIR when applied to raw material characterization in a test case using the Freiberg mine.

2 RGB Imaging and FTIR techniques

2.1 RGB Imaging

Red-Green-Blue (RGB) cameras operate in the visible range of the electromagnetic spectra and are commercially most mature technology with rapid data processing capability. RGB sensors are robust for environmental conditions, non-destructive, need no sample preparation and can be used for in-situ application. In addition, the technique is completely passive so it can be used in multiple environments. RGB sensors are manufactured by multiple suppliers as consumer digital cameras. Commercial availability is therefore not a concern.

RGB imagers characterize the reflectance property of a material and deliver 3 (red-green-blue) spectral band information often using three independent CCD sensors. As an alternative, some cameras capture the three band information using complementary metal oxide semiconductor (CMOS) technology. A RGB camera captures images using a line scan technique and a frame (area scan) sensor. To capture an image, frame cameras use a two-dimensional array of sensors. Line scan cameras have a 1 -dimensional array of sensors.

The technology has great potential for mineral/lithological mapping. It produces a multispectral image and can be used for identification of minerals and lithological units based on material colour or visual appearance. It produces images that can been seen by human eyes. The data becomes instantly understandable to viewers or operators e.g for a quality control application. RGB sensors are portable and so are easier for embedding and surface mounting. One potential such application is

side wall imaging at a mine face. In general, the technology can be directly applied in colour detection or indirectly for shape recognition of geological units.

Application of RGB images for material characterization is very limited, so far it is used in recycling, sorting and agricultural application. The use of high spatial resolution and colour selectivity, [5] revealed the application of the technology for mineral sorting such as sorting of talc and calcite. [6, 7] showed the potential of RGB images for automatic detection, classification of plant leaf diseases and crop monitoring. The technology can be used for colour sorting of different material streams and surface inspection of natural material [8]. However, application of RGB images for underground mine material characterization is poorly defined. This study addresses the potential of the technology for mine face mapping. In addition, the result was validated using FTIR technique.

2.2 Fourier-transform infrared spectroscopy (FTIR)

Infrared (IR) spectroscopy is a mature technology for the analysis of inorganic and organic materials[9-11]. When samples are exposed to infrared radiation, the bonds in the molecules selectively absorb the energy of the infrared radiation at specific wavelengths and this causes a change in vibrational energy level of the molecules. Signals in the infrared spectrum of materials are produced as a consequence of molecular vibrations. Vibration mode is different for each molecule that the infrared spectrum can be analysed to get information on different functional groups which further can be related to mineralogy.

The infrared region of the electromagnetic spectrum is divided in to Near Infrared (NIR: 0.7 – 1.4μm), Shortwave Infrared (SWIR:1.4– 2.5 μm), Mid Wave Infrared (MWIR: 2.5 - 7μm), Long Wave Infrared (LWIR: 7-15μm) and Far Infrared (FIR: 15 - 1000μm) regions. SWIR is commonly used for analysis of a wide range of alteration minerals. The LWIR region is used for identifying rock forming minerals. However, the MWIR region is the least explored region and it is the focal point of this study.

FTIR spectrometer has significant advantages of over other infrared spectrometers. It is a particular focus of this study. For example, FTIR spectroscopy has a higher signal to noise ratio (The desired signal to the level of background noise is higher so extracting signal is easier), higher accuracy, short scan time, high resolution and wider scan range [10, 12-14]. Moreover, current advances of the technology have produced portable FTIR spectrometers and the technology has a high potential for real-time (in-situ) application [13].

A FTIR analyser has integrated sampling interfaces; Diffuse Reflectance, Attenuated Total Reflectance (ATR) and External Reflectance to enable molecular spectra to be obtained with little or no sample preparation[13]. It is a non-destructive technique, it provides point data with high data frequency (measurement time less than 30 seconds) and enable infrared (IR) spectral analysis in a handheld package that it can be used for in-situ application in real-time basis. However, a protective cover is required for an underground application. The analyser works over a wide range of the electromagnetic spectrum (1.9μm - 14.0μm) that it is ideal for identification of various minerals.

Unlike other sensor technologies with a well-established spectral libraries (such as SWIR and RAMAN), the MWIR region of the FTIR spectra lacks well-developed libraries. This might be a chal-

lenge for direct interpretation of the spectral features. This study aims to explore the opportunities of FTIR combined with Chemometric techniques for material discrimination.

3 Study Area and Data acquisition

To assess the potential of RGB imaging and FTIR spectroscopy for raw material characterization, a realistic test case was chosen. This test case was chosen to be the Reiche Zeche underground test mine located in Freiberg, Germany.

3.1 Study Area

The Reiche Zeche underground mine is located in the eastern part of the Erzgebirge, Germany. It was mined for Silver, Copper, Lead and Arsenic (from 1168 to 1915) and later mainly for Zinc and pyrite [15]. Due to economic factors, the mine was closed in 1969. Starting from 1976, "Reiche Zeche" and "Alte Elisabeth" shafts were reconstructed as a research and teaching mine.

3.1.1 Geology

The Erzgebirge is part of the Mid-European metamorphic basement and it represents an antiformal megastructure. The antiformal megastructure has a large core which is constituted by medium to high grade metamorphic gneisses and mica schists with intercalations of eclogite [16].

In the Erzgebirge region, two main gneiss units are identified. These are "Red Gneiss Unit" and the "Grey Gneiss Unit". Based on textural differences, Grey Gneisses in the Eastern Erzgebirge (Freiberg mine area) have been subdivided into two groups [17, 18]: (1) Inner Grey Gneiss: coarse- and medium-grained biotite gneisses containing K-feldspar-porphyroblasts, and (2) Outer Grey Gneiss: mostly fine-grained biotite gneisses. The other rock types at the Freiberg mine include; mica schist, granulites, gabbro, variscan granites, variscan rhyolithes and eclogites [17]

3.1.2 Geological structures

The ore vein network in the test mine is characterized by two (NNE-SSW to N-S and E-W to ENE-WSW) shear systems, and spatially associated fissure veins [19]. In general, ores in the Freiberg mining district are associated with a system of dykes.

3.1.3 Mineralization

The Freiberg polymetallic sulphide deposit was formed by two hydrothermal mineralization events of Late-Variscian and Post-Variscian age [20]. The Late-Variscian mineralization event, which dominates in the central part of the mine, is rich in Sulphur, Iron, Lead, Zinc and Copper. Typical ore minerals are galena, pyrite, sphalerite, arsenopyrite, and chalcopyrite as well as quartz and minor carbonate gangue.

The Post-Variscian mineralization event is characterized by ore minerals with less Iron, Copper and Zinc. It consists of a fluorite-barite-lead ore assemblage, mainly comprising galena, sphalerite, pyrite, chalcopyrite and marcasite as well as quartz, barite, fluorite, and carbonates as gangue [20, 21]. The polymetallic sulphide veins of the base metal deposits in the Erzgebirge are hostetd by ortho gneiss (Freiberg district), mica schists (northern part of the Freiberg districts, Johanngeorgenstadt), and sub-ordinately by postkinematic granites (Schneeberg and eastern part of the Freiberg district).

For this study, ore implies the polymetallic sulphide deposits including Galena, Sphalerite and Chalcopyrite. Waste implies the gangue materials including carbonates, quartz and fluorite.

3.2 Data acquisition

Field work was carried out to define, image and map a selected mine face. This face was used to test the project concept. In addition, the test case material is characterized by a high material and mineralogical variability. A strategic sampling campaign was planned and conducted to generate reliable and usable data of appropriate accuracy and precision. The RGB images were taken *in-situ* and the FTIR measurements were performed in the laboratory using the samples acquired from systematic channel samples from the defined mine face.

3.2.1 RGB Imaging

The defined mine face has a lateral extent of ~ 22m and height ~2m, 42 reference points with 50cm spacing are marked horizontally at the mine face (Figure 2). RGB photographs are acquired at the defined mine face using Nikon D7100 digital camera with a focal length of 35 mm. The geographic coordinate of the 21 reference points with 1m spacing are acquired using LIDAR scan. Later, these points are used to georeference and mosaic the images. In addition, each image was taken at the specified 21 reference points. The full sets of images are acquired using the same camera setting.

The field of view of the camera varies depending on the distance between the camera and the mine face, effort has been made to ensure the same areal extent coverage during image acquisition. Most importantly, the images ensures to cover at least 3 reference points that these points can be used as Ground Controlling Points(GCP) to tie the images together. Taking in to account the approximate area coverage of each images, two vertical reference points were used to cover the whole defined face laterally and vertically (Figure 1 and Figure 2).

To avoid or minimize illumination effect, halogen lamps were used to ensure constant illumination condition throughout the mine face. To minimize distortion, the photographs were taken right in front of the face (~ 90^0). Photos have about 40% overlap that the defined face is fully captured and the images can be tied together. At each reference point 2 or 3 pictures were taken in case to avoid errors which can be associated with the photographing process.

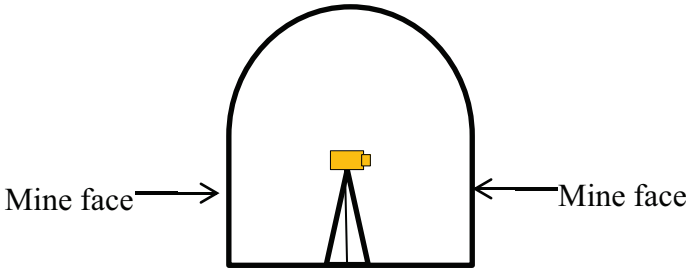

Figure 1: Sketch to illustrate the mine face cross section

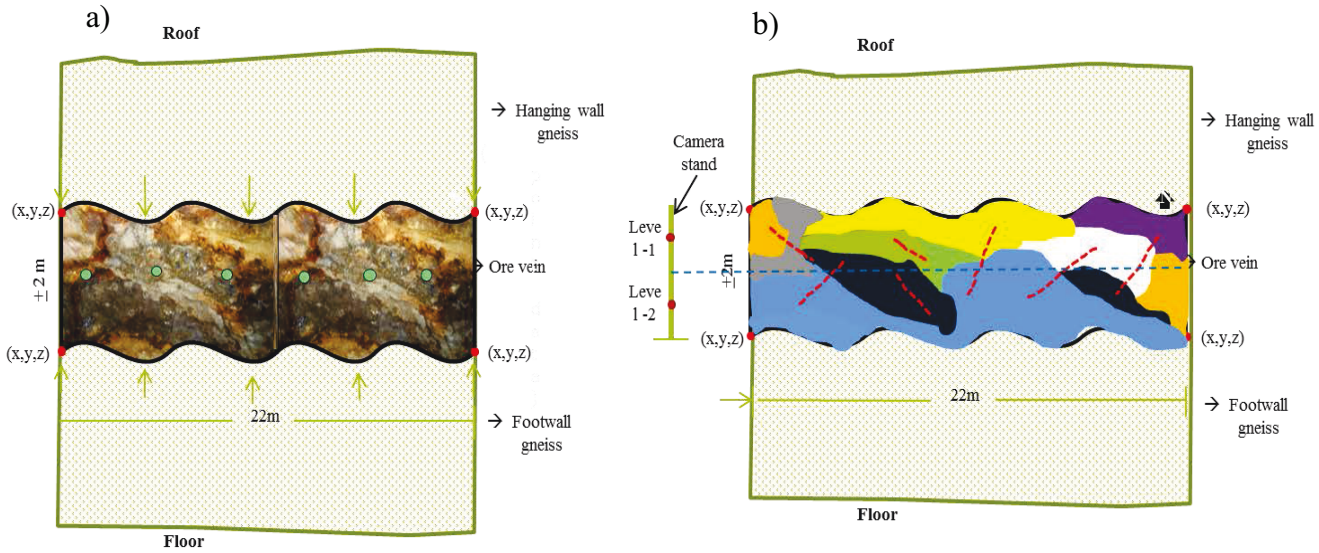

Figure 2: a) Overview illustrating the reference points and the defined mine face
b) Illustrates the two vertical reference points for imaging

A total of 42 images were acquired from the 21 horizontal and 2 vertical camera reference points. These images fully cover the defined mine face both laterally and vertically.

Physical samples were acquired to validate the RGB imaging. To ensure the representativity of the samples and to address the spatial variability over the 22m mine face, channel sampling was used. This samples each lithotype and ore type independently. A total of 23 channels were cut and about 102 samples were collected at different intervals of each channel Figure 3.

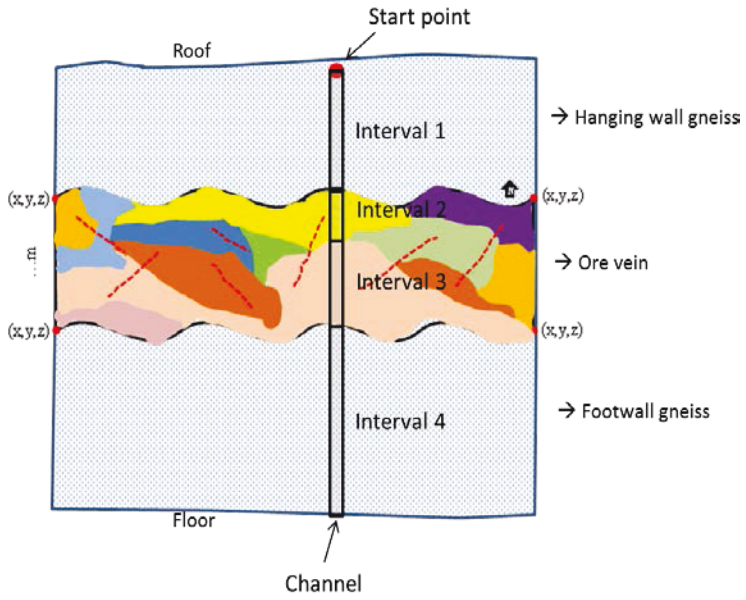

Figure 3: Sketch to illustrate the different intervals of a representative channel sample

3.2.2 FTIR

FTIR measurements were performed using the collected channel samples from the test site. Each channel sample is split in to two sample sets. One sample set comprises whole rock samples and the other half is pulverized to produce powder samples. The test case samples are heterogeneous, so multiple spectra were collected from each sample in order to accommodate the degree of heterogeneity within the samples. FTIR data is collected using powder and rock samples. The result presented in this paper shows the FTIR measurements using powder samples.

The geological nature of the deposit defines the material properties and such properties that are relevant for sensor-based material characterization. The choice of sensor and type of sensor measurements need to be optimized for mineralogical and material features of a specific deposit type. The FTIR measurements were optimized for the test case materials by considering different FTIR setups. Such optimization includes interfaces (Attenuated Total Reflectance (ATR), External reflectance and Diffuse reflectance), number of sample scans, calibration time and resolution. The ATR sampling interface measures the internal reflection. External reflectance measures the specular reflection from the sample surface. It is usually most applicable for smooth surfaces. Diffuse reflectance measures both internal and external reflection. It is usually associated with reflection from rough surfaces and is most relevant for this study.

The performance of the three sampling interfaces for materials from the test case was checked for both whole rock and powder samples. A variety of sample scans were tested and the influence of this on the measurement result was checked. To acquire better signal to noise ratio different calibration times of the instrument and the number of background scans was assessed. The instrument acquires data at different resolutions. To assess the validity, measurements were collected at 4cm-1, 8cm-1 and 18cm-1 resolutions and the results are compared.

This work presents the results of analysis of 170 FTIR spectra collected with the preferred instrument set-up. Each spectra represents 64 sample scans at 4cm^{-1} resolution and over a spectral range

of ~2.5 µm to ~15µm. To ensure maximum signal to noise the background reference was conducted over 126 scans.

4 Methodology

4.1 RGB Imaging

The RGB images were acquired from the two vertical reference points (illustrated in Figure 2b) and a total of 42 images were acquired to cover the defined ~22m lateral extent of the mine face. This study presents the result of 8 images which cover ~ 5m laterally and ~ 2m in height. The GCP's were used to georeference and mosaic the images together. The coordinate transformation was done using a similarity polynomial (a first order polynomial which preserves shapes). To enhance distinct identification of feature types, pre-processing and classification of the RGB images were carried out. The major steps followed are presented in Figure 4.

Categorical classification using both unsupervised and supervised classification techniques were used. First, unsupervised classification (UC) using k-mean methods were applied to assess any clustering or grouping of pixels based on their grey level. The k-mean method is one of the most commonly used and efficient UC method for cluster analysis. It assigns n observations into k clusters using the centroid of the clusters and minimizes the sum of squared error [29]. UC is done with no *apriori* knowledge about the different classes however it requires *apriori* specification of the number of cluster centers. This part is considered as part of exploratory data analysis.

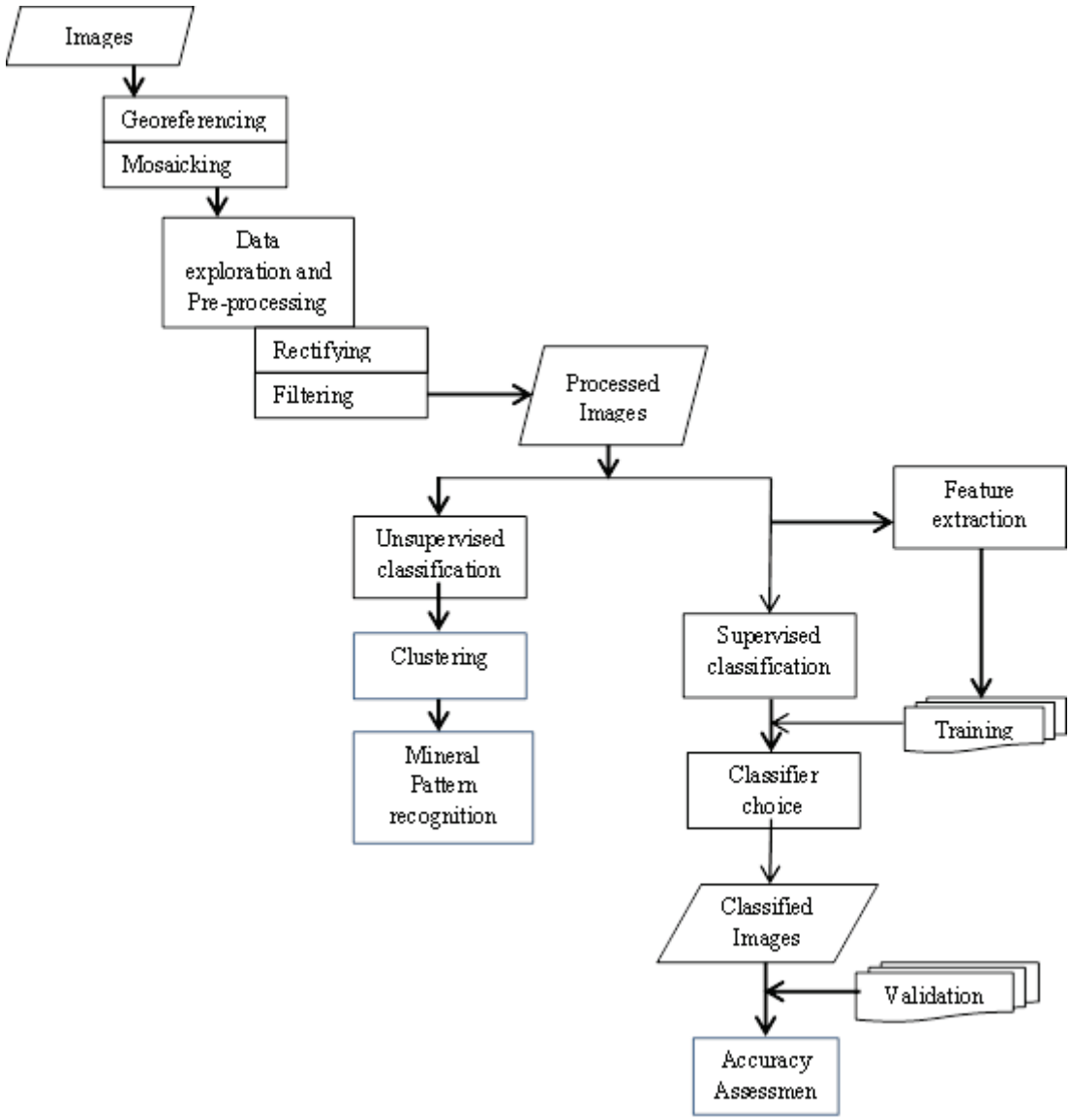

Figure 4: Workflow for RGB image processing and information extraction

Supervised classification requires a training set for the classifier. The classifier uses a training set of spectral signatures to identify of similar signatures in the remaining pixels of the images. It labels all the image pixels as per the trained parameters [22]. Prior knowledge of the different classes is crucial since the training set selection affects the classification accuracy. A large number of supervised classification algorithms are available for image classification and the choice of the classifier algorithm is based on classification accuracy [22, 23]. For this study, the classification performance of Maximum likelihood (ML), Minimum distance (MD) and Spectral Angle Mapper (SAM) algorithms were compared.

The ML computes the probability of each pixel belonging to a class which is represented in the signature file and assigns the pixel to its most probable class. ML is based on two principles; one is that the distribution of each class is normally distributed and uses Bayes' theorem to assign the pixels in to classes [24]. The MD classifier uses the training data to determine the means of a class and classify unknown pixels to classes of nearest means [24]. The SAM classifier considers the set of reference spectra (training data) and the unknown pixels as vectors, and calculates the spectral angle between them to identify the different classes in the image[25].

Visual interpretation of the RGB images was conducted to identify the main mineral classes within the defined mine face. The visual inspection of the images was supported by the geological map which was generated during the sampling campaign. Training sets (groups of pixels) were generated to represent five broad classes in a supervised classification. The feature selection is based on the visual appearance (colour difference) of the designated material classes. The number of mineral types which can be identified depends on different factors, such as: the presence of the minerals at certain location, their clear appearance, the freshness of the exposure so that oxidation or other weathering processes will not lower the visibility of the minerals and the resolution of the camera. Thus, for some of the pictures more than 5 mineral classes are identified.

To ensure reliable prediction of the class membership, training area uniformity and representability of the same class over the whole image was taken in to account. In addition, separability of the classes in the multidimensional attribute space was checked using histograms. Overlapping classes were merged together and five broad classes were identified for the classification. Some of the minerals are combined together (e.g quartz and calcite) since distinguishing the minerals based on their colour and the utilized camera resolution is limited.

Following the selection of training areas a signature file was generated and the whole image was classified using the signature file of the training sets. The output multiband raster is a classified image which shows the mineral distribution at the defined mine face. The classification work is validated using a separate validation sample set.

4.2 FTIR

FTIR spectroscopy combined with techniques used for chemometrics were used to investigate the applicability of the technology for the discrimination of the test case materials in to ore, host rock and weathered materials. Examples of each are illustrated in Figure 5. Chemometrics or multivariate data analysis involves mathematical and statistical methods to process data and understand the chemical compositional information of a material [26, 27]. The multivariate data analysis approach include: design of experiment, explanatory data analysis and predictive or classification model development. The design of experiment was developed for both independent and combined preprocessing strategies Figure 6. Principal Component Analysis (PCA), outlier detection using T^2 hostelling and loading plot interpretation was carried out to explore the dataset and gain knowledge.

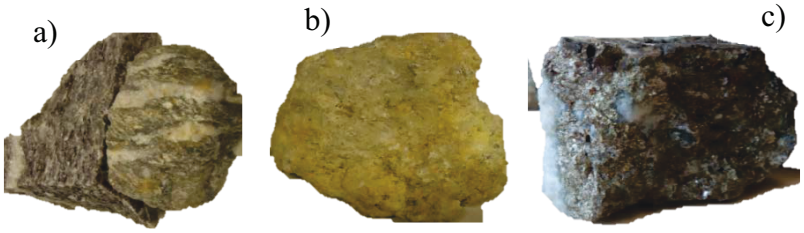

Figure 5: Rock samples representing the three material classes
a) Gneiss, b) Weathered material c) Sulphide ore

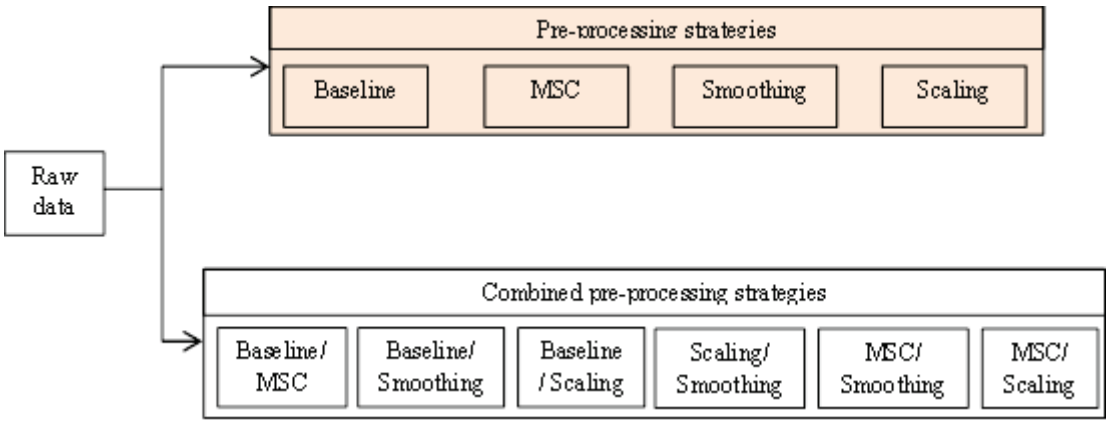

Figure 6: Design of experiment for both independent and combined pre-processing strategies

The explanatory data analysis includes an assessment of descriptive statistics and the PCA model. PCA alone does not provide much, however it orders the latent variables and is useful for visualization of high dimensional data. The most important question is how to distinguish between noise and signal (how to extract valuable information or real information). Therefore, there is a need for design of experiment for different data pre-processing strategies independently or in combination and to apply a discriminant analysis to distinguish the most informative variables. The goal of data pre-processing is to remove data artefacts and make the data more amenable for data analysis. Many data pre-processing methods are available. In this study, the following methods were applied independently and in combination; baseline correction, Multiplicative scattering effect (MSC), smoothing (such as Gaussian filter smoothing) and scaling (such as normalize and Standard Normal Variate (SNV)).

A Partial Least Square - Discriminant Analysis (PLS-DA) classification model was developed to find a discrimination rule for different categories. PLS-DA is a supervised classification method, which builds classification rules (model) for pre-specified classes. PLS-DA is useful to identify key variables for class separation and it helps in understanding differences among groups of samples. Later, the model can be used for assigning unknown samples to the most probable class. Data is prepared for PLS-DA analysis; category variables are converted into indicator variables. These indicator variables are the Y-variables in the PLS model. The PLS-DA was performed in two steps; first PLS regression was performed and later prediction. PLS regression was performed using the dependent /response variable (Y) and the categorical data (the different classes). So, three PLS-DA models (one for each class) were developed. The technique is a one versus all approach which uses a binary encoding; it assigns 1 if the unknown measurement belongs to the specified class or 0 if it belongs to other classes (Figure 7). Since three classes are considered, Y (the output) is a matrix where binary encoding is used for pre-specified 3 classes (the number of targets). The length of Y will be the same as the number of samples in X.

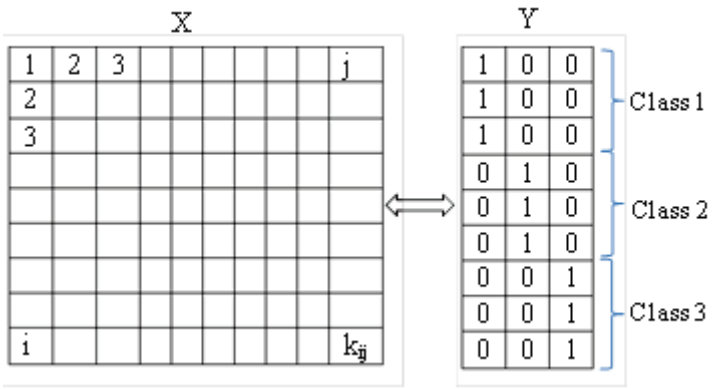

Figure 7: A sketch to demonstrate PLS-DA model for three classes. X denotes the input data where i is the number of samples, j is the number of variables

Model validation is a key requirement for all modelling tasks. Accordingly, to ensure proper model performance and assess the model's variable ranking, validation was carried out. To perform the validation, the datasets were randomly split in to training and test sets taking in to account approximately equal presence of each classes in the training (calibration) and test (validation) set. The random split of the datasets is to avoid systematic error. The calibration data has 130 measurements and the validation data has 40 measurements. For a direct comparison of the MWIR and LWIR data outputs, the calibration and validation data were obtained from identical samples measurements. The parameters of the model are estimated using the training set and the performance of the model was evaluated using the test set.

The FTIR data was acquired over the range of ~1.9µm to ~15µm wavelength. However for samples from the test case the range from 1.9 µm to 2.5 µm gave a noisy result and was excluded from all further analysis. Then, the spectral range from 2.5µm to 15µm was split into MWIR (2.5 - 7µm) and LWIR (7 - 15µm) regions. Thus, the capability of the two datasets for the discrimination of the test case materials was assessed separately. The whole data was acquired first and later split. Therefore, for the two regions data is basically collected using the same setup and the same sample. MWIR is the least explored region due to limited instrument development. Therefore, there are few reference spectra. Thus, it is an exciting area of development which shows potential for discrimination of minerals. Compared to MWIR, LWIR is a better explored region of the IR. Instruments which operate over this region are available such as: hyperspectral imaging. This region can be used for identification of rock forming minerals, specifically silicates.

First, using the design of experiment, the MWIR and LWIR spectra were pre-processed using independent and combined data filtering techniques. The class discrimination after each filtering technique was assessed. Later, PLS-DA was applied for each pre-processed data and the performance of the models was evaluated.

5 Results and Discussion

5.1 RGB imaging

RGB images are acquired *in-situ* and georeferenced/mosaicked together using the GCP's marked on the mine face. Georeferencing and mosaicking of the RGB images is advantageous; to comprehend the full spatial distribution of minerals (spatial variability) on a single image, gives extended or full area coverage of the mine face, to generate spatially constrained image data which further can be linked with other sensor outputs based on location and improve positional accuracy of data.

The output of unsupervised classification using k-mean is used to determine the general pattern/ groups of the different classes with minimum degree of heterogeneity within a class (Figure 8). This is considered as the first step for image classification since unsupervised classifiers might be useful for discovering unknown but useful classes [28]. In addition, the classified image was used as a preliminary input for definition of the training set.

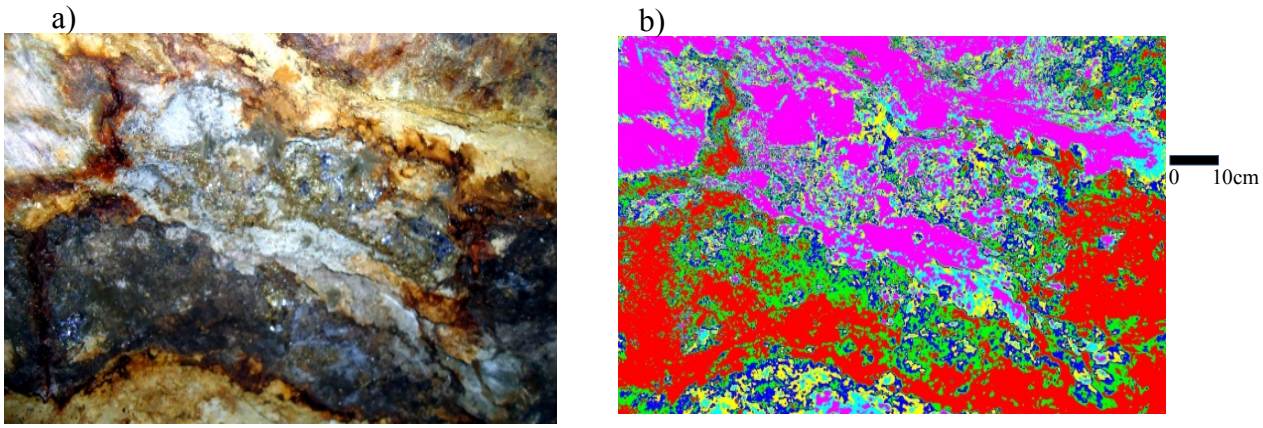

Figure 8: a) RGB image b) Thematic map produced by K-mean classifier

Using the same training set the accuracy of ML, MD and SAM classification methods were compared. The classification results were examined visually (pattern match) and validated. As can be inferred from Figure 9, a better pattern match was achieved using ML. The classifier choice was optimized using a single image at a time but tested on multiple images. Once the preferred classifier is selected it was applied to the mosaicked images.

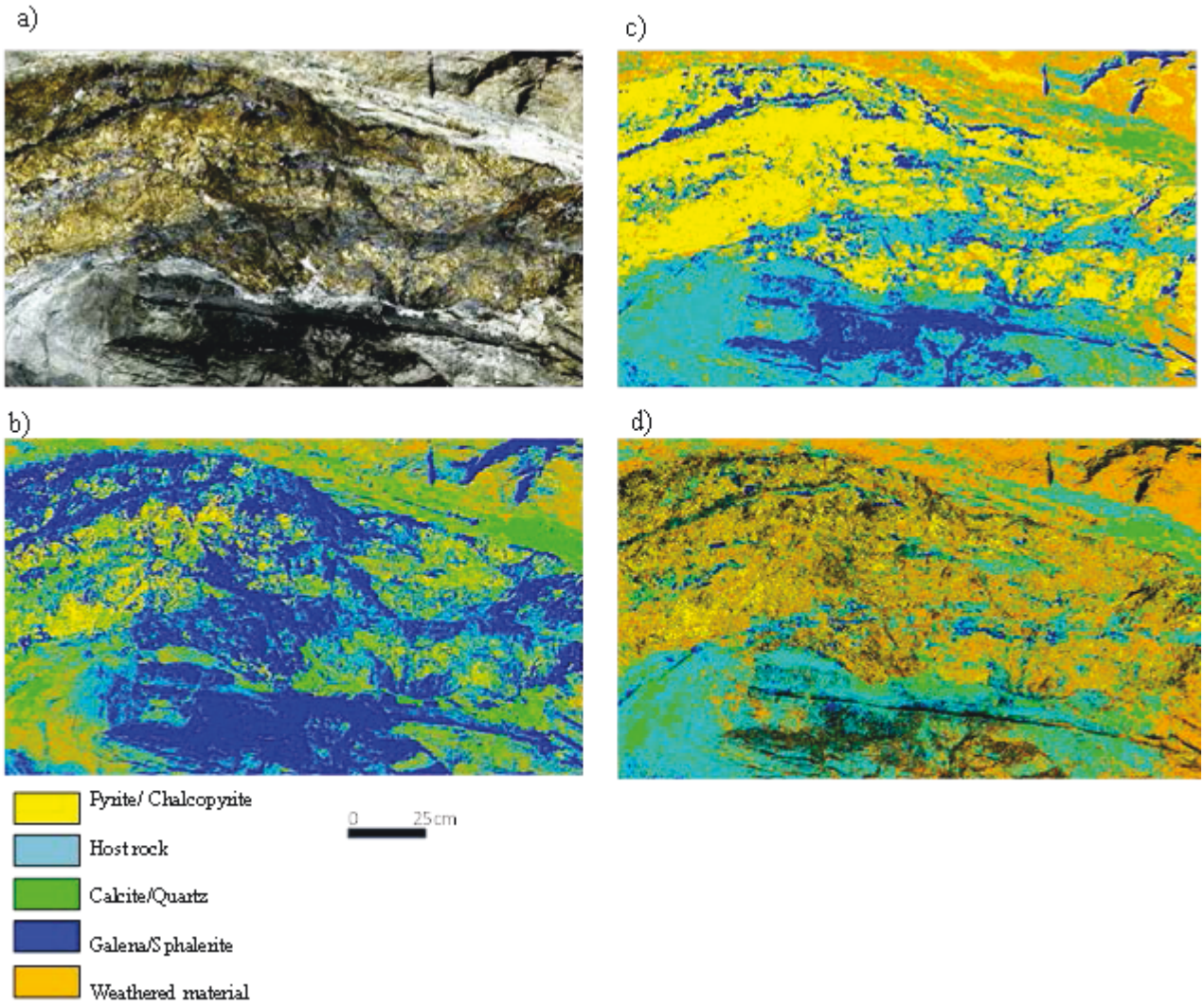

Figure 9: a) RGB image taken at the test case mine face. Ore zone delineation results produced by three classifiers b) MD c) ML d) SAM

Figure 10 shows an RGB image of the polymetallic sulphide ore at the mine face. The classifier identified, 6 main classes (mineral types). The classification algorithm performance was assessed using a validation set. The acquired overall accuracy is 78% and the class accuracy increases to 94%.

Most sulphide minerals show sufficient variation in colour (and therefore can visually be differentiated by their colour) that they can be delineated or mapped using RGB images. However, the same mineral (e.g quartz) can appear in different visual appearances depending on its context so the training set definition should take in to account the visual appearance of minerals in specific deposit types. Taking this in to account, the colour of typical minerals from the test case was inspected prior to feature selection. In the test mine, Arsenopyrite has silvery/golden colour , Pyrite has golden appearance, Galena is grey, Sphalerite is dark grey to black and Quartz is white in colour . This visual characteristic of the minerals makes RGB imaging a potential technique for the delineation of sulphide ore zones based on their colour.

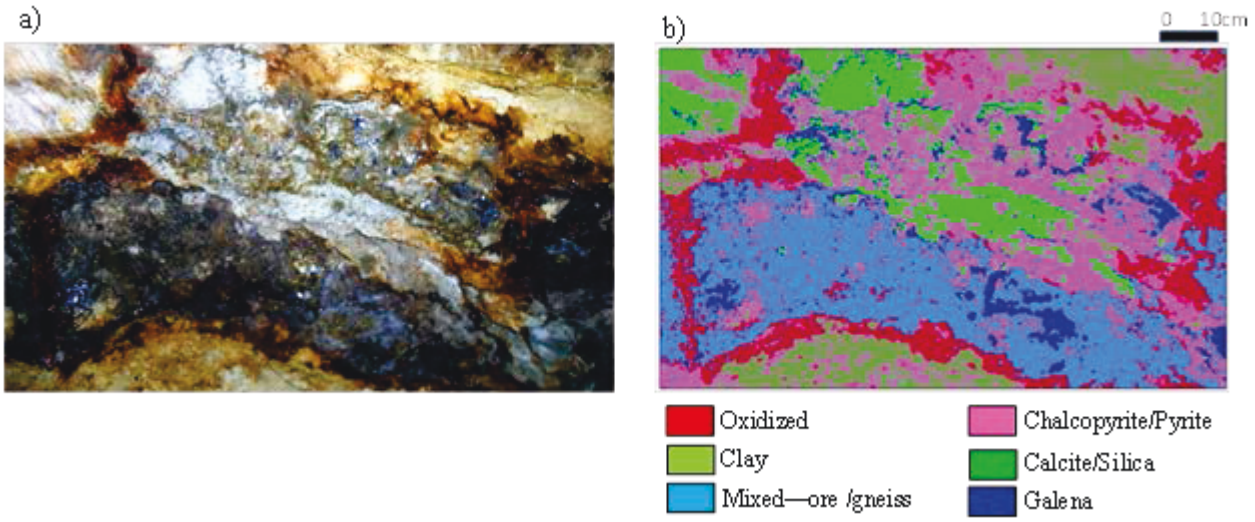

Figure 10: a) shows an RGB face image taken from polymetallic ore at the Freiberg mine
b) Mineral map produced from RGB image

The classification work was extended for georeferenced and mosaicked images. This is illustrated in Figure 11. These images are taken at a different location but at the same mine face such that the spatial distribution of the minerals is different. Figure 11 shows 8 images tiled together and classified using the same training set. The inset picture shows the reference points across the ~22m long mine face and the location of these 8 images relative to the reference point. Since, images were not taken immediate after blasting, the visibility of the sulphide minerals is reduced due to weathering. As a result, differentiation among sulphide minerals was not achieved. However, image pixels were successfully classified into five mineral classes namely weathered material, ore, quartz/ calcite , ore disseminated in gneiss and gneiss. This is a good input to map a high grade ore zone and low grade ore zone.

The acquired overall classification accuracy (78%), spatial or positional accuracy of the georeferenced images ($\pm$6cm), spatial resolution (336µm) and easy interpretability of the classification results makes RGB imaging a potential technique for ore zone delineation. Imaging is advantageous since it covers a wider areal extent and gives information at each specific point on the image. Whereas, point spectrometers such as Laser Induced Breakdown Spectroscopy (LIBS) or IR (e.g ASD point analyser) gives point data at specific locations. Compared to other techniques such as hyperspectral imaging, acquisition of RGB images is low cost, low data volume and low computational intensity technique. For the same deposit type, if illumination is kept constant over the imaged mine face, the same training set can be used to automate the classification process. In addition, an RGB imager is a rapid, easily repeatable data acquisition system and it has a good potential for automation.

Moreover, the use of a base map is important for geological or mineralogical mapping, however a base map for sidewall mapping maybe difficult to obtain. This might raise a scale issue for mapping of different lithological and structural units. RGB imaging can be a solution. Due to depletion of minerals, the future mine is likely to shift to deeper environments. In such conditions it is not conducive to stay longer to undertake extensive geologically mapping work. RGB imaging offers a potential automated solution. Moreover, mapping in deleterious or hazardous environments can also be achieved using RGB imaging. In general, comparing the approach with conventional mapping

methods; RGB imaging gives objective, reproducible results and an expandable database. It can be considered as complementary technique for mineral mapping.

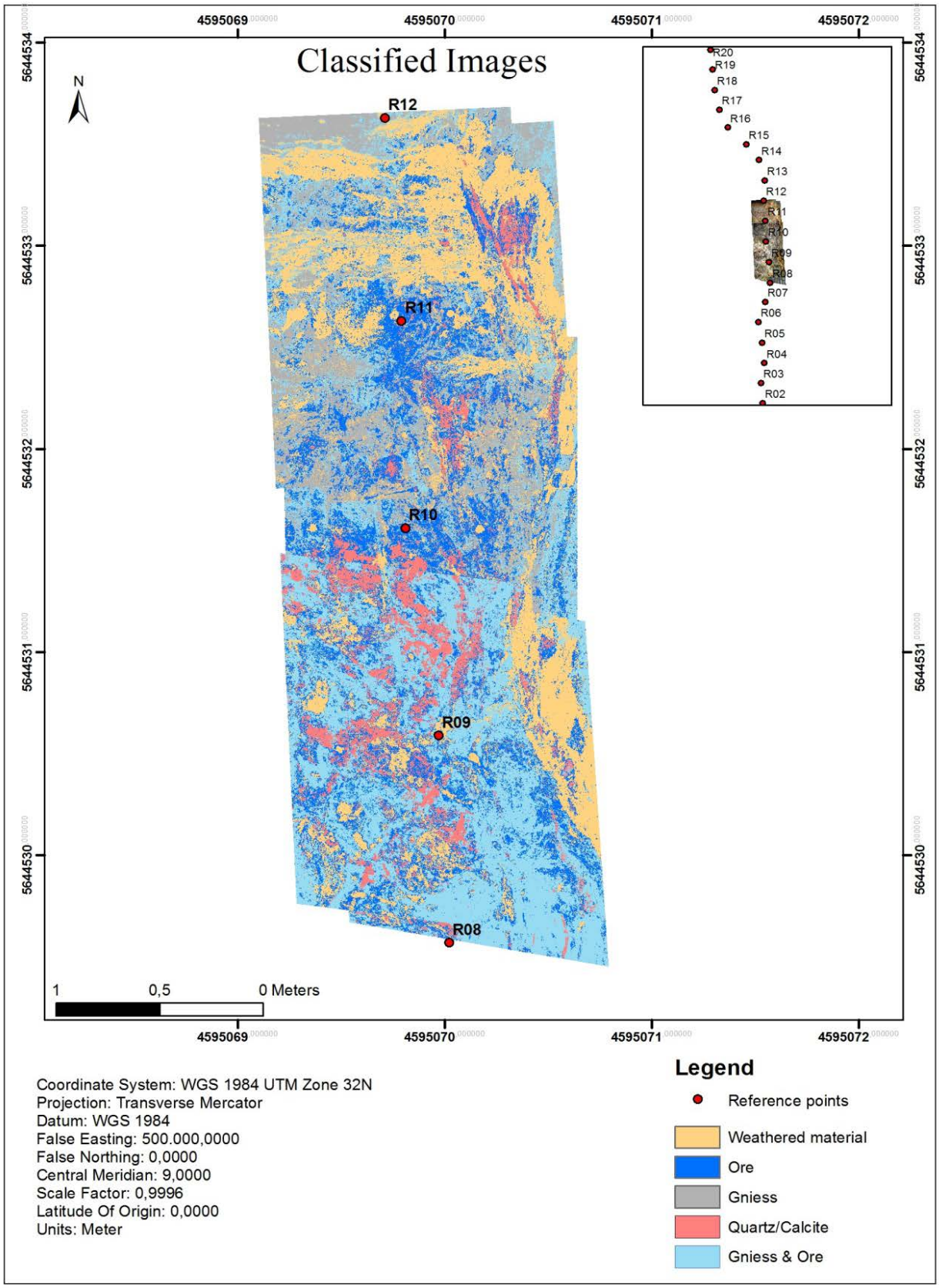

Figure 11: Thematic map of the mosaicked images. The relative location of the classified images with respect to the 22m mine face is indicated in the inset map

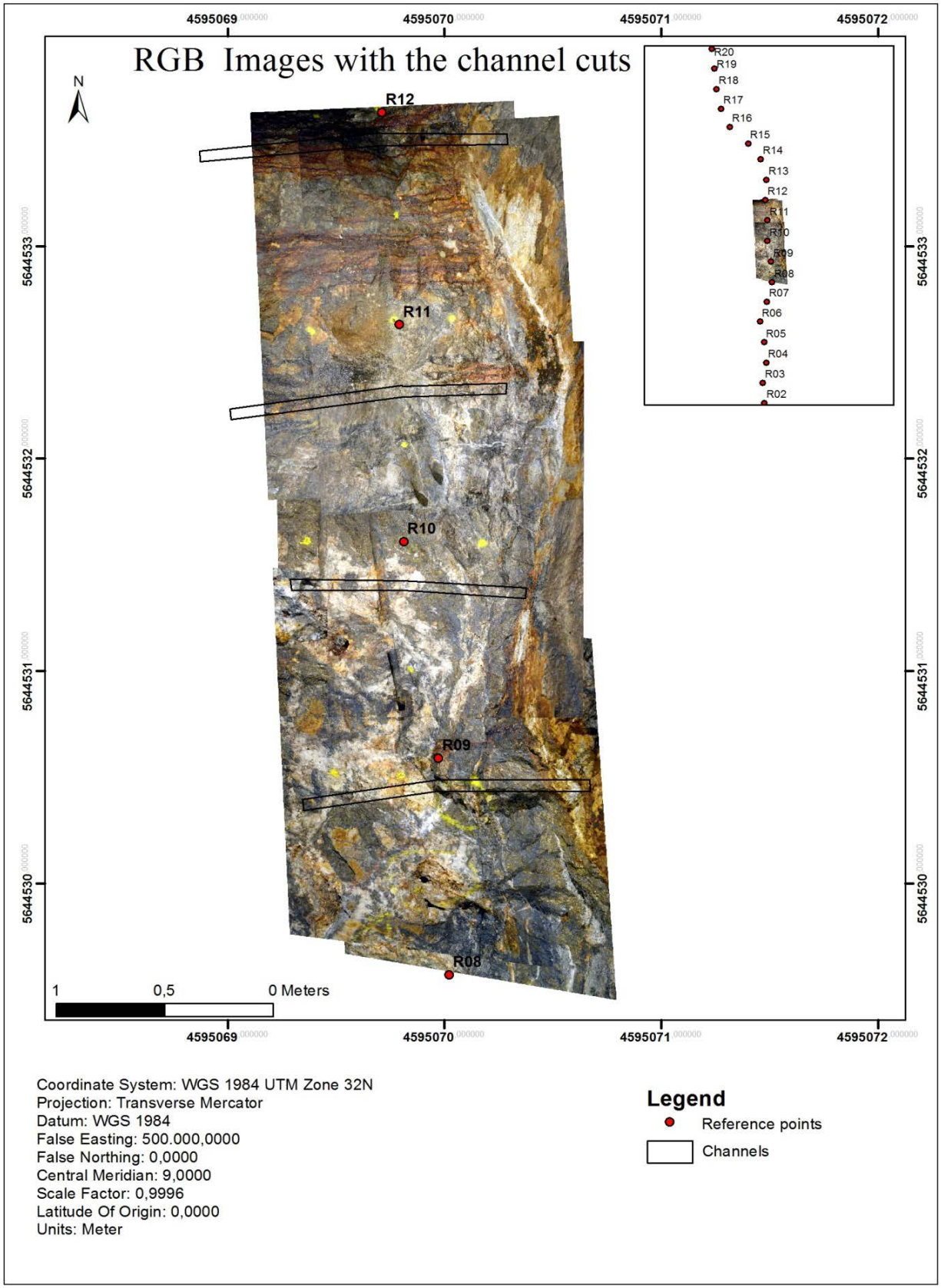

Figure 12: Mosaicked RGB images showing the position of the channel samples superimposed. The channels have ~80 cm to 120 cm spacing. Channel locations with their corresponding intervals were digitized from the images. Thus, samples acquired from the channels were spatially constrained.

Channel samples were acquired from the mine face. The face was imaged after the channels were cut and the location of each channel was digitized from the images. This is shown in Figure 12. This is advantageous for generating spatially constrained/ controlled data which will have a significant input for testing sensor technologies, sensor data integration based on location, for clear understanding of the spatial distribution of minerals (which will have an important implication for interpretation of sensor outputs) and to provide location based sensor output data for resources model updating.

5.2 FTIR

A total of 170 spectra were collected and the data were fused into a single matrix for multivariate data analysis. Based on the design of experiment, independent and combined data filtering techniques were applied to the data. Later, a PLS-DA classification model was developed to assess the discrimination results of the raw and processed data. Figure 13 shows PCA models for MWIR and LWIR after data scaling. As can be inferred from the figure each material type is clustered together but the boundaries are not that clearly defined.

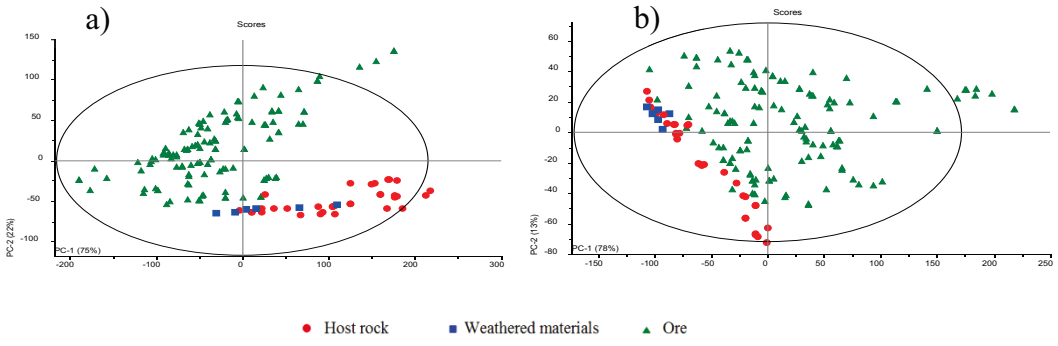

Figure 13: PCA distribution of a) MWIR data b) LWIR data of the three material types

The ellipse which bounds the data points on the graph (hostelling's T^2), shows the possible outliers of the dataset. Outliers can be due to measurement error or a unique sample measurement result. Their variability is poorly described by a model. Thus, the observed outliers are excluded from the dataset in order to ensure proper description of variables by the model.

Figure 14 shows the score plots of the MWIR and LWIR data after the data is treated with independent and combined filtering techniques. The score plots show the data structure and sample differences or similarities in relation to each other. Compared to the raw data, a better clustering and clear boundaries are achieved for MWIR data after the data is processed. LWIR data shows an improvement after data pre-processing is applied. However, the class separability is clearer for the MWIR data than the LWIR data. The LWIR data do not differentiate the host rock from weathered materials.

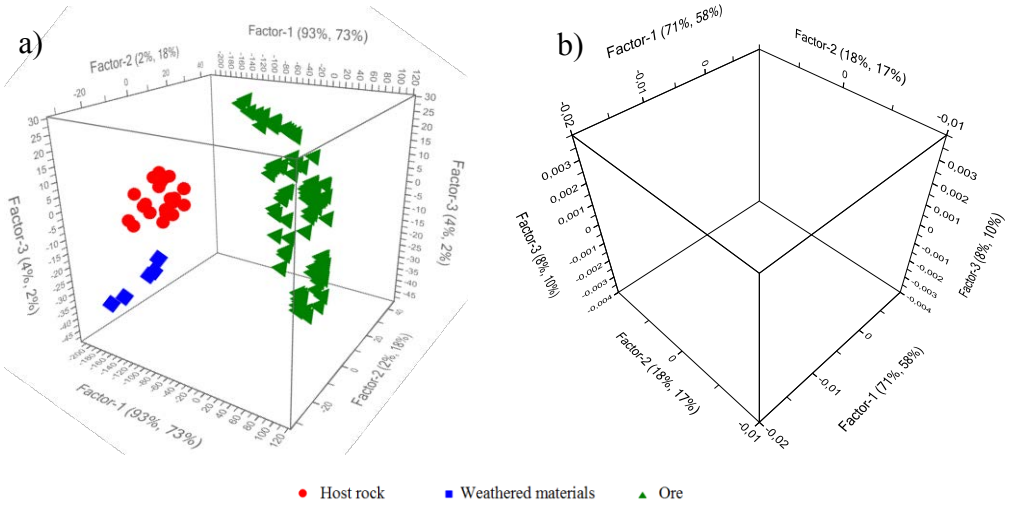

Figure 14: The score plots of the first three factors from PLS model a) MWIR data after baseline correction is applied to the data b) LWIR data after Gaussian and Normalize data filtering is applied to the dataset

The PCA model was used to transform the full spectra into latent values (PC's), later the loading plot of the PC's was interpreted to select the important variables for class differentiation. The first 3 PC's explained 99% and 96% of the variation for MWIR and LWIR data respectively. The loading plot of the first 3 PC's are shown in Figure 15 and Figure 16. Regions indicated by orange coloured squares are informative variables in the spectral data which are responsible for the difference between the samples. For purpose of clarity, not all important variables are indicated. As can be inferred from Figure 15 large loading coefficients (most variation) are observed for the MWIR data from 2895 – 2300 cm-1 (3.45 – 4.3µm) and 1985 – 1581cm-1 (5 – 6.3 µm), so these region are the most informative region for the class differentiation since variation equal information. There is a clear difference among the three classes (Figure 14a) that the selected variables are valid to distinguish the three classes.

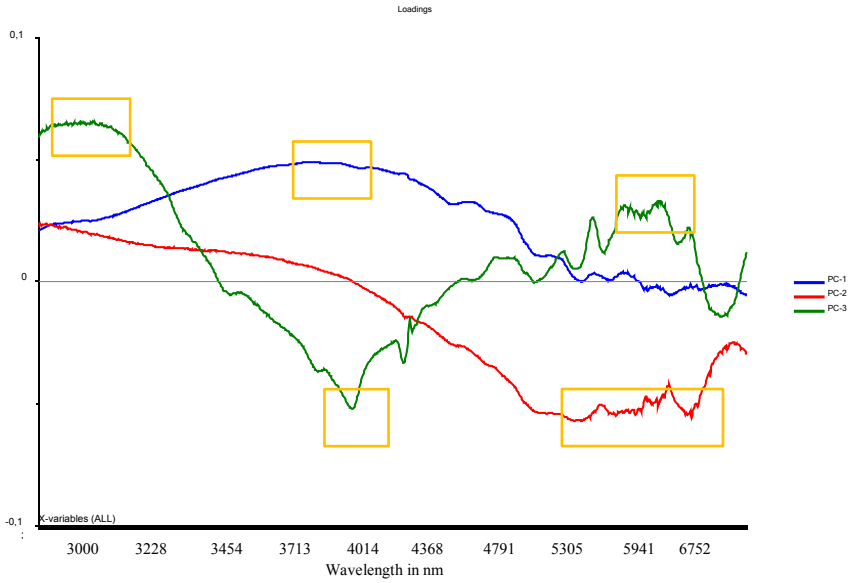

Figure 15: The loading plot of the first 3 PC's of the MWIR data

Figure 16 shows the loading plot for the first 3 PC's of LWIR data. Variables with large loading coefficients are observed at 7µm, 8.2 µm, 8.9 µm, 9.5 µm 10.7 µm and 13µm. Thus, these variables are responsible for the observed differences between the samples or have a large influence for the differentiation. This might explain why LWIR could not differentiate weathered material from the host rock, since most of the variation is in region from 8.2 µm to 9µm where quartz is a prominent feature in this region. This might be because the concentration of quartz in Gneiss and the weathered products (relatively quartz is resistant to weathering) is higher than the quartz content in the ore.

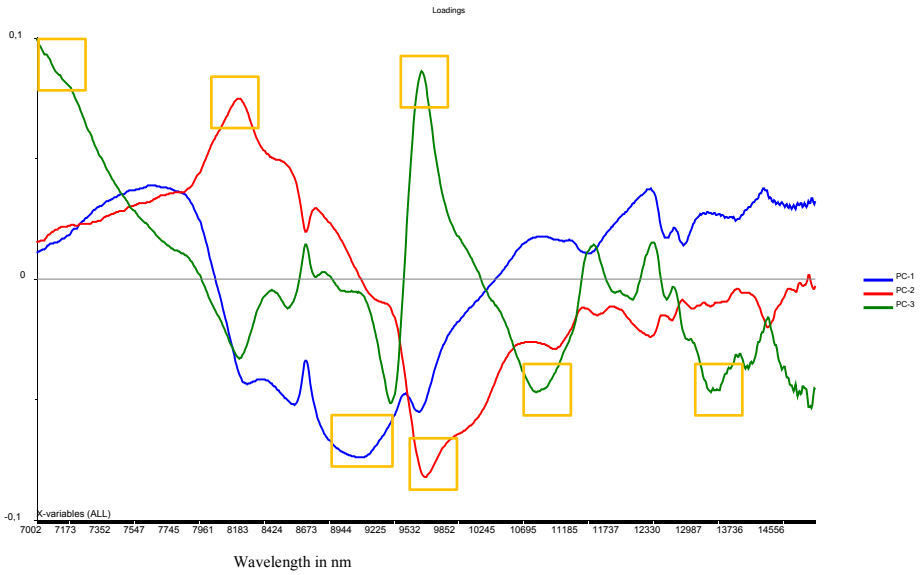

Figure 16: The loading plot of the first 3 PC's of the LWIR data

Later, the pre-procced data were used to develop classification models using PLS-DA. The accuracy of the results were compared for the different independent and combined filtering techniques Table 1.

Table 1 : PLS-DA model calibration and prediction statistics for ore prediction

Filtering techniques	RMSECal		RMSECV		RMSEP		R^2	
	MWIR	LWIR	MWIR	LWIR	MWIR	LWIR	MWIR	LWIR
Raw data	0.19	0.21	0.21	0.23	0.21	0.19	0.71	0.78
SNV	0.077	0.12	0.09	0.15	0.08	0.14	0.96	0.886
Baseline	0.1	0.13	0.11	0.155	0.09	0.15	0.95	0.87
MSC	0.11	0.14	0.13	0.19	0.134	0.22	0.895	0.72
Gaussian	0.09	0.15	0.097	0.166	0.074	0.16	0.97	0.85
Combinations								
Baseline/SNV	0.097	0.12	0.109	0.114	0.098	0.133	0.944	0.898
MSC/ Baseline	0.099	0.125	0.12	0.21	0.13	0.194	0.9	0.78
Baseline/normalize	0.08	0.11	0.087	0.13	0.09	0.11	0.95	0.93
Gaussian/SNV	0.08	0.12	0.09	0.14	0.082	0.14	0.96	0.886
Gaussian /normalize	0.076	0.089	0.08	0.1	0.09	0.09	0.954	0.95
Gaussian / baseline	0.085	0.11	0.09	0.145	0.07	0.142	0.97	0.88
Gaussian / MSC	0.11	0.13	0.13	0.19	0.133	0.17	0.897	0.84

As is inferred from Figure 14 and Table 1, for this specific dataset MWIR data provides more accurate discrimination results compared to LWIR data. Independent and combined data filtering techniques were employed to evaluate the performance of the processed data for the discrimination of the three classes. For each data processed with either independent or combined filtering techniques, the calibration statistics and model prediction statistics show that generally the RMSE values are lower and the R2 values are higher for MWIR data than LWIR. This indicate that the discrimination capability of MWIR data is superior to LWIR data. However, for both datasets the discrimination capability was enhanced by employing the filtering techniques. The result is interesting since MWIR is the least explored region in terms of material characterization, and this region shows the potential of the MWIR data for discrimination of these materials.

Considering a single filtering technique, the MWIR data gives a better discrimination result after the data is treated using Gaussian filter smoothing while baseline correction resulted in a better discrimination result for LWIR data. In general, a better discrimination results were achieved after both datasets are processed using the filtering techniques. However not all filtering techniques necessarily improve the model performance. For example, for the LWIR dataset, MSC filtering technique does not improve the result while baseline correction gave an improved result. This might arise from the fact that multiplicative effect is not pronounced in the data.

Comparing the single filtering techniques with combined filtering techniques, technique combination resulted in improvement of the discrimination results for LWIR data. The maximum accuracy was achieved when Gaussian filter smoothing is combined with area normalization. However, combination of the filtering techniques did not improve the accuracy of discrimination results for

MWIR data. In general, accuracy of the discrimination result varies from technique to technique. Therefore, the design of experiment is a crucial step to choose the best suited filtering technique for each specific dataset.

Sub-clustering of minerals within the general ore class was observed. This sub-clustering might be attributed to the different ore minerals which occur in the ore since ore is likely composed of multiple minerals. Thus, the approach can further be extended for discrimination within the ore minerals with careful model calibration and using an extended dataset.

In addition, this experiment was tested by categorizing the materials into two classes; ore verses waste. The waste material comprises both the host rock and the weathered material. Here, equal numbers of samples were used in both categories. As it can be inferred from the score plot of PLS model Figure 17, it is possible to categorize the samples in two classes. Using the FTIR spectral data combined with data filtering techniques the discrimination results of the PLS-DA model can be improved.

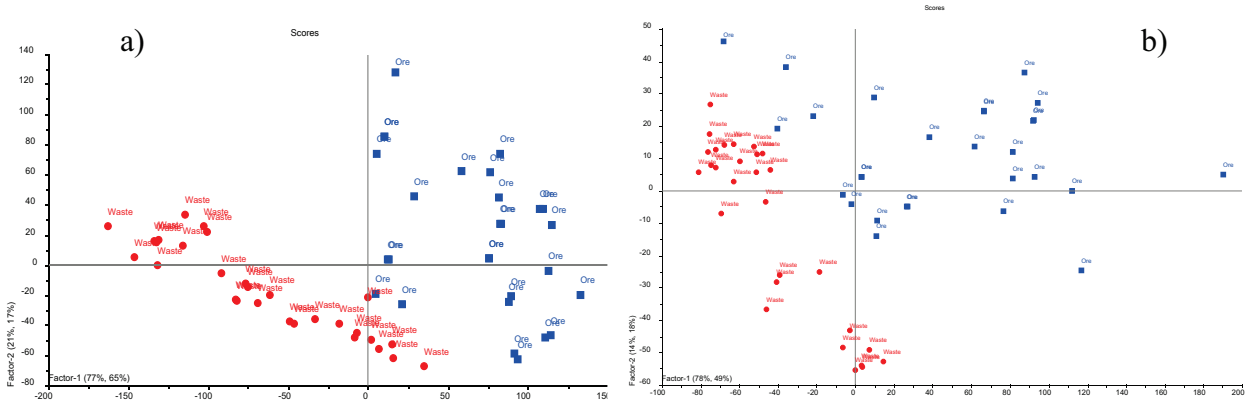

Figure 17: Score plots for equal class size a) MWIR b) LWIR data

6 Conclusions

This study focused on investigating the characterization of samples from the test case utilizing RGB imaging and FTIR technology combined with chemometric methods. A well-defined imaging procedure was developed to acquire RGB images at the defined mine face. Later, the images were georeferenced, mosaicked and a mineral map was produced using a supervised image classification technique. The supervised image classification identified, 5 main classes (mineral types) with overall accuracy of 78%. The result shows that the approach is efficient and provides acceptable classification success for delineation of a polymetallic sulphide ore zone in an underground mine at this specific site. Compared to the conventional mapping methods, RGB imaging gives automated, reproducible and objective results. Moreover, RGB imaging systems are easy to use, rapid, low-cost and robust to environmental conditions. The technology shows good potential for mapping of visually distinct minerals in underground mines.

FTIR measurements were optimized for the test case materials and data were acquired using the preferred instrument setup. Later, the FTIR data was split in to two datasets, one covering the MWIR region and the other covering the LWIR region. Design of experiment was implemented in order to identify optimal specific and combined pre-processing strategies for discrimination of the

three classes (ore, weathered material and the host rock) using both datasets separately. The discrimination result shows remarkable improvement after a pre-processing strategy was applied to the dataset. Furthermore, using the processed data PLS-DA discrimination models were developed and the predictive abilities of the models were evaluated by the calibration and prediction statistics in the form of an estimated prediction error. The results demonstrated that (for the tested datasets) the MWIR data shows a better discrimination result than the LWIR data. Loading plots were interpreted and important variables (wavelength location) responsible for the discrimination of the three materials type were identified. This could be an important input for identification of minerals using FTIR spectra. Using FTIR combined with chemometrics it is possible to classify the test case material. With more FTIR spectral data and accurate model calibration, the approach can be extended for automation of the material discrimination process.

REFERENCES

1. Benndorf, J., Buxton, M.W.N., 2016. Sensor-based real-time resource model reconciliation for improved mine production control – a conceptual framework. Mining Technology. **125**(1): p. 54-64.

2. Buxton, M.W.N., Benndorf, J., 2013. The Use of Sensor Derived Data in Optimization along the Mine-Value-Chain An Overview and Assessment of Techno-Economic Significance, in International Congress of the ISM 2013. p. 324-336.

3. Fox, N., Parbhakar-Fox, A., Moltzen, J., Feig, S., Goemann,K., Huntington, J.,2017, Applications of hyperspectral mineralogy for geoenvironmental characterisation. Minerals Engineering. 107: p. 63-77.

4. Goetz, A.F.H., Curtiss, B., Shiley, D.A.,2009. Rapid gangue mineral concentration measurement over conveyors by NIR reflectance spectroscopy. Minerals Engineering. **22**(5): p. 490-499.

5. Tomra. Mining sorting solutions. 2017 [cited 2017 18-8]; Available from: https://www.tomra.com/.

6. Singh, V., Misra, A.K., 2017. Detection of plant leaf diseases using image segmentation and soft computing techniques. Information Processing in Agriculture. **4**(1): p. 41-49.

7. Valentine L.[1], Agnes B. [2], Sylvain L. [3], Benjamin M. [2], Laurent P. [4], Bruno R. [5], 2008. Can Commercial Digital Cameras Be Used as Multispectral Sensors? A Crop Monitoring Test. Sensors (Basel, Switzerland). 8 p. 7300-7322.

8. LLA Instruments GmbH. 2017. Real-time color analysis for machine vision and sorting applications. [cited 2017 18-8]; Available from: http://www.lla-instruments.com/spectrometer-cameras/RGB-line-scan-camera.html.

9. Griffiths, P.R., Haseth, J.A.,2007. Fourier Transform Infrared Spectrometry. 2nd Edition ed. WILEY-INTERSCIENCE.

10. Smith, B.C.,2011. Introduction to Infrared Spectroscopy, in Fundamentals of Fourier Transform Infrared Spectroscopy, Second Edition. CRC Press. p. 1-17.

11. Chukanov, N.V., Chervonnyi, A.D., 2016. Infrared spectroscopy of minerals and related compounds. Springer: Cham.

12. Chemistry libretexts. 2017. How an FTIR Spectrometer Operates. [cited 2017 July 5]; Available from: https://chem.libretexts.org/Core/Physical_and_Theoretical_Chemistry/Spectroscopy/Vibrational_ Spectroscopy/Infrared_Spectroscopy/How_an_FTIR_Spectrometer_Operates.

13. Agilent. 2017. FTIR Compact & Portable Systems. [cited 2017 February 2]; Available from: http://www.agilent.com/en/products/ftir/ftir-compact-portable-systems/4300-handheld-ftir.

14. Perkins, W.D., 1987. Fourier transform-infrared spectroscopy: Part ll. Advantages of FT-IR. Journal of Chemical Education. **64**(11): p. A269.

15. Silberstadt Freiberg. 2015. Freiberg Exhibition Mine (Besucherbergwerk Freiberg). Available from: http://www.freiberg-service.de/en/highlights/sightseeing/freiberg-exhibition-mine.html.

16. McCann, T., 2008. The Geology of Central Europe: Volume 1: Precambrian and Palaeozoic. Geological Society, London, Geology of Series.: Geological Society of London.

17. Tichomirowa, M., Berger, H. J., Koch, E. A., Belyatski, B. V., Götze, J., Kempe, U., Schaltegger, U., 2001. Zircon ages of high-grade gneisses in the Eastern Erzgebirge (Central European Variscides) -constraints on origin of the rocks and Precambrian to Ordovician magmatic events in the Variscan foldbelt. Lithos. **56**(4): p. 303-332.

18. Willner, A.P., Rotzler, K., Maresch, W.V., 1997. Pressure-Temperature and Fluid Evolution of Quartzo-Feldspathic Metamorphic Rocks with a Relic High-Pressure, Granulite-Facies History from the Central Erzgebirge (Saxony, Germany). Journal of Petrology. **38**(3): p. 307-336.

19. Scheinert, M., Kupsch, H., Bletz, B., 2009. Geochemical investigations of slags from the historical smelting in Freiberg, Erzgebirge (Germany). Chemie der Erde - Geochemistry, **69**(1): p. 81-90.

20. Seifert, T.,2008. Post-Collisional Magmatism and Its Relationship to Late-Variscan Ore Forming Processes in the Erzgebirge (Bohemian Massif). Germany: Technische Universitat Bergakademie Freiberg.

21. Benkert, T., Dietze, A., Gabriel, P., Gietzel, J., Gorz, I., Grund, K., Lehmann, H., Lowe, G., Mischo, H., Schaeben, H., Schreiter, F., Stanek K.,2015. First step towards a virtual mine - generation of a 3D model of Reiche Zeche in Freiberg. GiGa Infosystems, TU Bergakademie Freiberg.

22. Kaufman L., Rousseeuw P.J., 2005. Finding Groups in Data: An Introduction to Cluster Analysis. John Wiley & Sons; Hoboken.

23. Kotsiantis, S.B., 2007. Supervised Machine Learning: A Review of Classification Techniques. Informatica, **31**: p. 249-268.

24. Richards, J. A., 2013. Remote Sensing Digital Image Analysis, in Supervised Classification Techniques. Springer-Verlag Berlin Heidelberg.

25. Richards, J.A., Jia, X., 2006. Remote Sensing Digital Image Analysis. 4th Edition ed.

26. George P. P. [1,2], Krishna, P. V. [3], Gavriil, X. [4], George,K.[5], Marko,S. [1], 2010. A Comparison of Spectral Angle Mapper and Artificial Neural Network Classifiers Combined with Landsat TM Imagery Analysis for Obtaining Burnt Area Mapping. Sensors (Basel, Switzerland).

27. Brereton, R.G., 2007. Applied Chemometrics for Scientists, in John Wiley & Sons Ltd.

28. Roussel, S., Preys, S., Chauchard, F., Lallemand, J., 2014. Multivariate Data Analysis (Chemometrics), in Process Analytical Technology for the Food Industry, C.P. O'Donnell, C. Fagan, and P.J. Cullen, Editors., Springer New York: New York, NY. p. 7-59.

29. Jain, A.K., Murty, M.N., Flynn, P.J., 1999. Data clustering: a review. ACM Comput. Surv., **31**(3): p. 264-323.